

## Airborne measurements of UV spectral actinic radiation with CCD spectroradiometers – applications aboard Zeppelin NT and the research aircraft HALO

Insa Lohse and Birger Bohn

Institut für Energie- und Klimaforschung 8: Troposphäre, Forschungszentrum Jülich GmbH, Jülich, Germany

**Abstract.** Airborne measurements of spectral actinic flux densities (280-650 nm) were performed using two spectroradiometers each covering a  $2\pi$  field-of-view. A method was developed to compensate for the non-ideal combined angular response of the optical receivers, based on spectral radiance distributions from radiative transfer calculations. Correction factors on the order of 1-3 % were derived dependent on atmospheric conditions. First results of aircraft campaigns with a Zeppelin and the research aircraft HALO are presented.

### Introduction

Ultraviolet solar radiation is driving atmospheric chemistry because the photolysis of trace gases yields highly reactive atoms or radicals. Photolysis frequencies ( $j$ -values) are first-order rate coefficients quantifying photolysis processes in the atmosphere:

$$j = \int_{\lambda_1}^{\lambda_2} \sigma(\lambda)\phi(\lambda)F_{\lambda}(\lambda)d\lambda. \quad (1)$$

In this equation  $F_{\lambda}$  is the solar spectral actinic flux density,  $\sigma$  is the absorption cross section of the absorbing molecule and  $\phi$  is the quantum yield of the photo-fragments. Spectroradiometry is the most versatile method to measure  $F_{\lambda}$ . Airborne measurements require high flexibility, high time resolution, and a  $4\pi$  field-of-view. We used two single-monochromator-based CCD array spectroradiometers with identical receiver optics, each covering a  $2\pi$  field-of-view above and below the aircraft.

### Calibration and stray light correction

Spectral sensitivity calibrations were made in the laboratory using irradiance standards taking into account the characteristics of actinic radiation receivers (Hofzumahaus et al., 1999; Bohn et al., 2008). In addition, secondary standards were used during the aircraft campaigns. Since measurements with single-monochromators can be affected by stray light, cut-off filters were used to remove the influence on calibration factors. Stray light typically showed a linear behaviour in the cut-off range that was extrapolated and subtracted at all wavelengths. The same method was applied for atmospheric measurements where stratospheric ozone acts as a natural cut-off filter.

### Receiver angular response

Goniometric measurements were made in the laboratory to obtain the angular response functions  $Z_p(\lambda, \vartheta, \phi)$  of the actinic receiver optics. A typical dependence of  $Z_p$  on polar

angle is shown in figure 1. For  $\vartheta \leq 90^\circ$  deviations from the ideal response are small. At  $\vartheta > 90^\circ$  there is a small, inevitable cross-talk to the opposite hemisphere caused by the vertical extension of the ovoid receiver. For ground-based measurements of down-welling radiation this cross-talk is insignificant because of typically little upwelling radiation that can be further suppressed by horizontal shadow rings. However, for aircraft operations the situation is different. Because the combined  $4\pi$  response shown in figure 2 exhibits a distinct peak towards the horizon, a condition dependent correction is required to compensate this non-ideal response.

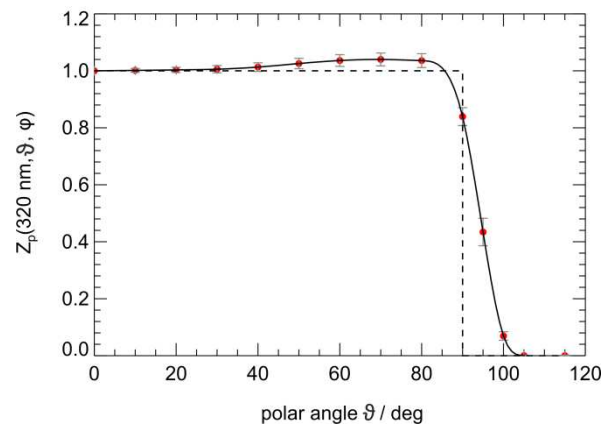


**Figure 1.** Relative angular response  $Z_p$  of a receiver for hemispheric measurements of actinic flux densities. The error bars indicate variations caused by different azimuth angles. The dashed line shows the ideal response of an actinic flux receiver. Wavelength is 320 nm.

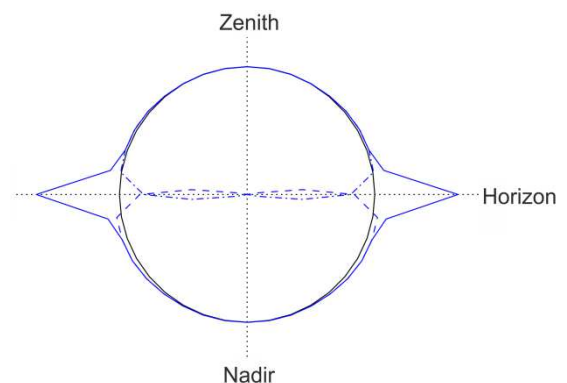


**Figure 2.** Relative angular response of a combination of two hemispheric receivers for airborne measurements. The dashed and dashed-dotted lines are the sensitivities of the nadir- and zenith-viewing receivers, the solid lines the sensitivity of the combined system. The black circle indicates ideal behaviour.

## Correction factors

Dimensionless correction factors  $Z_H$  were derived for various atmospheric conditions, flight heights and receiver combinations. The  $Z_H$  are based on calculations of atmospheric spectral radiance distributions  $L_\lambda(\vartheta, \varphi)$  performed with the libRadtran radiative transfer model (Mayer and Kylling, 2005) and the measured  $Z_p$  for each receiver:

$$Z_H = \frac{\int_0^{2\pi} \int_0^\pi Z_p(\vartheta) L(\vartheta, \varphi) \sin(\vartheta) d\vartheta d\varphi}{\int_0^{2\pi} \int_0^\pi L(\vartheta, \varphi) \sin(\vartheta) d\vartheta d\varphi}. \quad (2)$$

$Z_H > 1$  indicates an overestimation of actinic flux densities,  $Z_H < 1$  an underestimation.  $Z_H$  factors can also be defined separately for the upper and lower hemispheric measurements. The model was run under variation of the following input quantities: aerosol optical depth, surface albedo and flight height. Figure 3 shows examples of the dependence of  $Z_H$  on solar zenith angle for different flight heights and surface albedos. In all cases the actinic flux density is slightly overestimated by the measurements. The implementation of clouds is in progress.

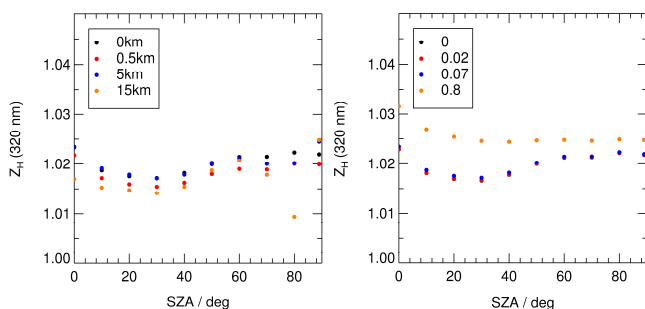


**Figure 3.** Dependence of  $Z_H$  on solar zenith angle for different flight heights (left) and surface albedos (right). Wavelength is 320 nm;  $\tau_{550\text{nm}} = 0.2$ ; ozone column = 300 DU; albedo=0.07 (left); height=0 km (right).

## Aircraft campaign data

Corrected  $F_\lambda$  were used to calculate photolysis frequencies according to equation (1). Measurements were performed in the atmospheric boundary layer on a Zeppelin during the PEGASOS campaign 2012/13 over different parts of Europe and in the free troposphere and lower stratosphere on the research aircraft HALO over the Atlantic Ocean during the 2013/14 NARVAL campaign. As an example, figure 4 shows an overview of all  $j(\text{O}^1\text{D})$  data obtained during the PEGASOS south campaign 2012 in the area of Bologna, Italy.  $j(\text{O}^1\text{D})$  is the rate coefficient of the UV-B photolysis of  $\text{O}_3$  leading to electronically excited  $\text{O}^1\text{D}$ . An overview of the data from the NARVAL south campaign is given in figure 5. Flights were performed from Germany to Barbados and back and in the area of Barbados.

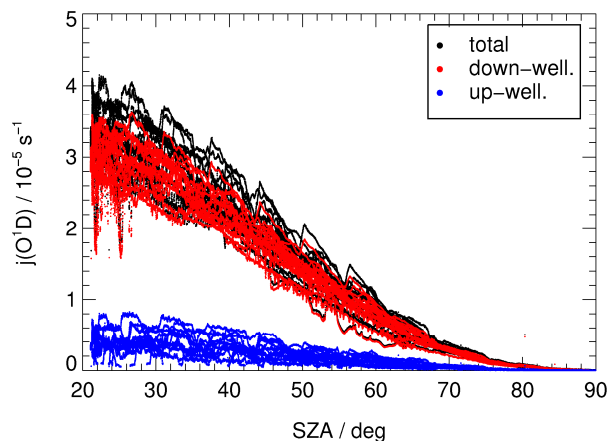


**Figure 4.** Overview of  $j(\text{O}^1\text{D})$  values obtained during PEGASOS (June-July 2012). Typical flight altitude was 400 m above ground.

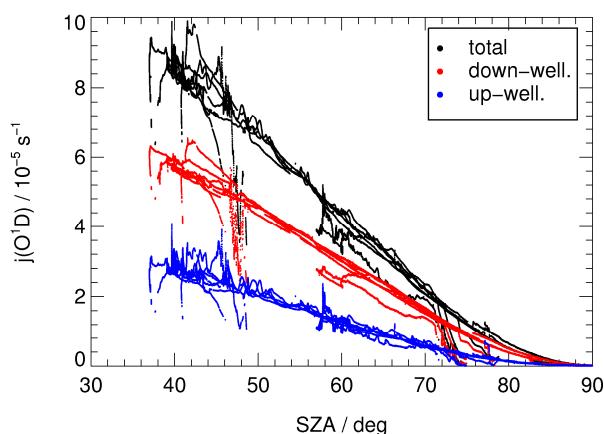


**Figure 5.** Overview of the  $j(\text{O}^1\text{D})$  values during NARVAL (December 2013). Typical flight altitude was 14 km. Note the different scale compared to figure 4.

## References

- Bohn, B., G. K. Corlett et al., 2008: Photolysis frequency measurement techniques: Results of a comparison within the ACCENT project. — *Atmospheric Chemistry and Physics*, **8**, **17**, 5373–5391.
- Hofzumahaus, A., A. Kraus and M. Müller, 1999: Solar actinic flux spectroradiometry: A technique for measuring photolysis frequencies in the atmosphere. — *Appl. Opt.*, **38**, **21**, 4443–4460.
- Mayer, B. and A. Kylling, 2005: Technical Note: The libRadtran software package for radiative transfer calculations - description and examples of use. — *Atmospheric Chemistry and Physics*, **5**, **7**, 1855–1877.

Acknowledgement: This work was supported by EC integrated project PEGASOS, Contract Number 265148 and the DFG project BO 1580/4-1.